... In Relation To Underlying Mantle Lithosphere Removal

Z. Saleeby, J. Saleeby, L. Le Pourhiet, and M. Gurnis

...with our thanks to the Gordon and Betty Moore Foundation

Figure 12. Early and middle Miocene paleogeographic map showing extension of San Joaquin basin across current Sierran uplift and resolved position of shelf edge. Basin subsidence, extensional faulting and volcanism are attributed to the migration of a slab window beneath the region during this time interval.

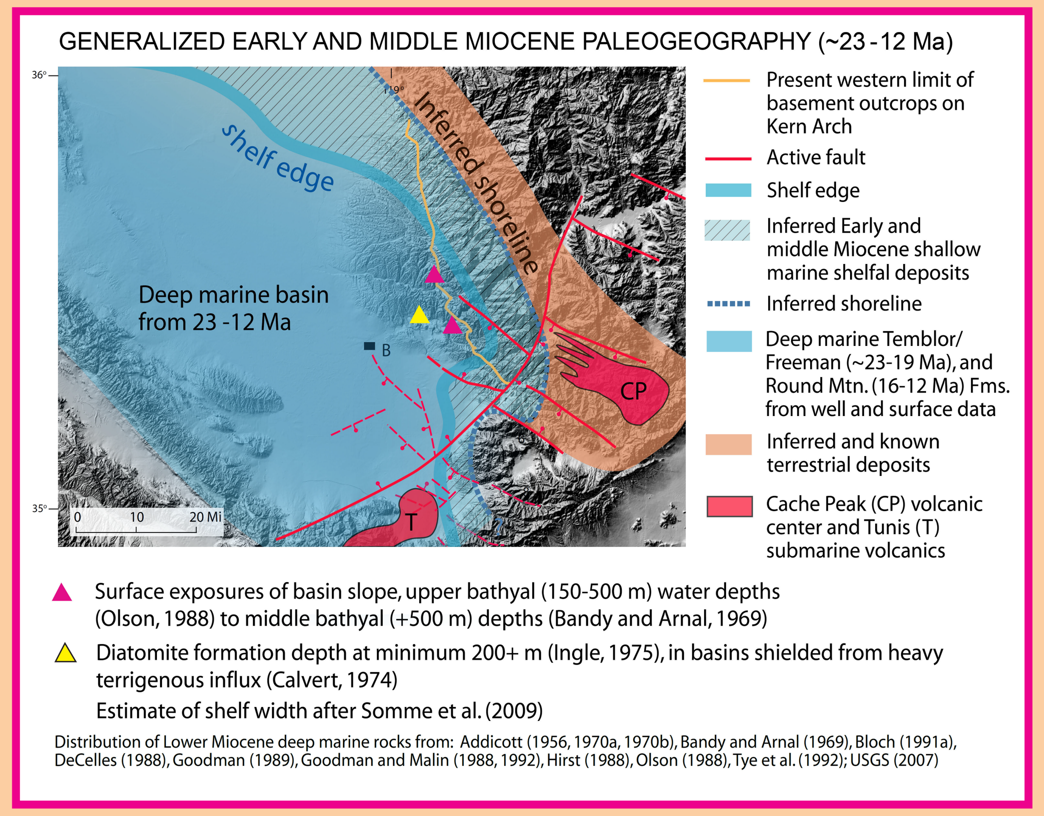

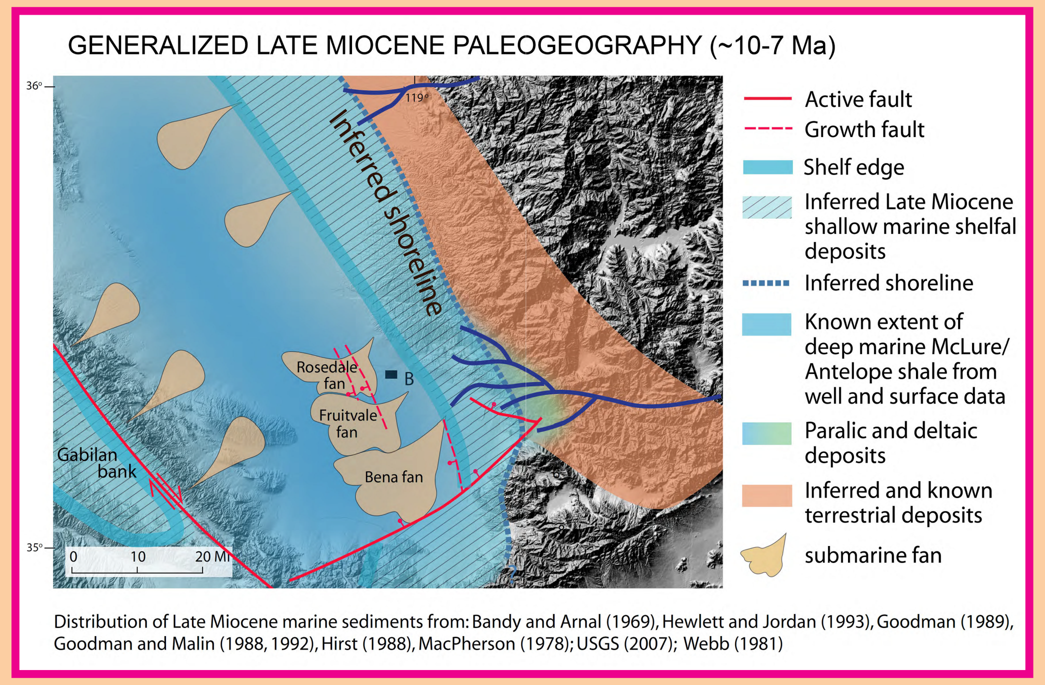

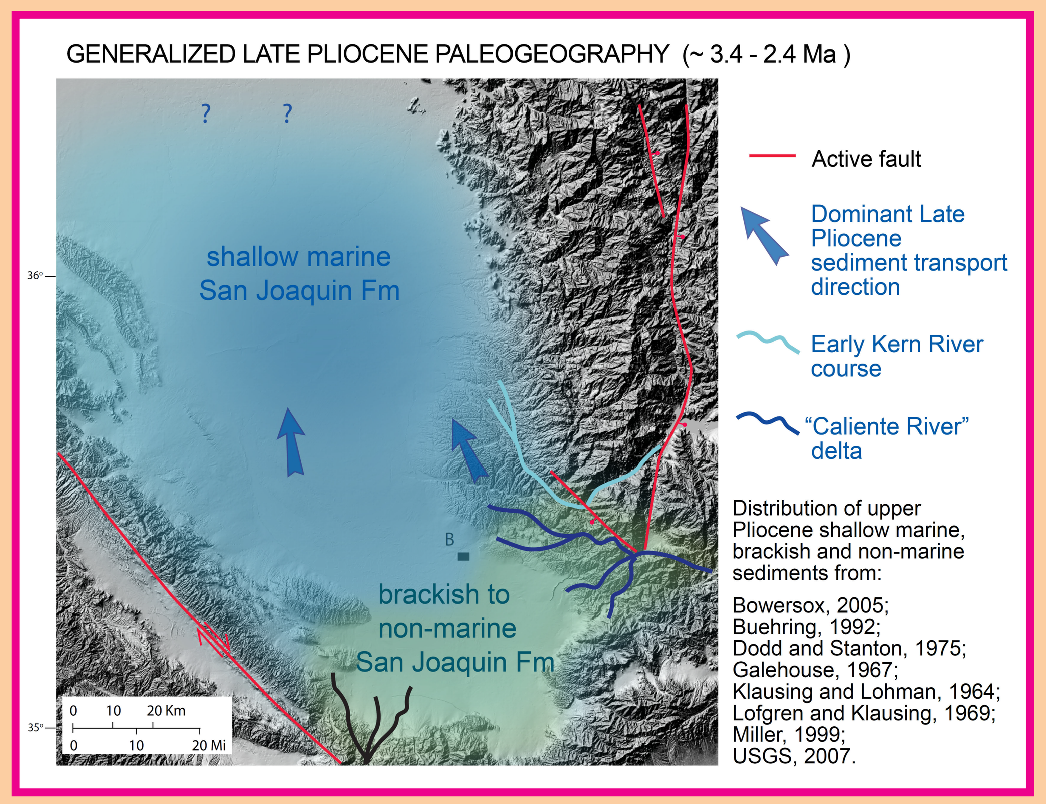

Figure 14. Late Pliocene paleogeographic map showing a major change in the principal San Joaquin basin depocenter from the southern Kern Arch-Maricopa basin to the northern Kern Arch-Tulare basin. These changes resulted from mantle lithosphere delamination as displayed in Figures 17-20.

PALEOGEOGAPHIC RECONSTRUCTIONS

Figures 12-14 are paleogeographic maps for the southwestern Sierra-SJB region covering early and middle Miocene (12), late Miocene (13) and late Pliocene (14). Note the extension of the eastern basin margin eastwards across the current Sierran uplift. Early and middle Miocene time was characterized by the northward migration of a slab window into the region in conjunction with the migration of the Mendocino Triple Junction. Initial migration saw a regression from Freeman-Jewett silt to Olcese sand, followed by subsidence in Round Mountain silt time (Fig. 7). Round Mountain subsidence was also characterized by high-angle normal faulting developed across the southern Kern Arch and intensified southward into the Maricopa basin (Fig. 2). In the late Miocene there was a major change in regional topography during the consolidation of the eastern Sierra normal fault system (see Fig. 18 below), resulting in regional west-tilting throughout the Sierra Nevada. At this time there was a major regression resulting in the deposition of the regional Santa Margarita beach sand sheet (Fig. 7), followed by the progradation of deltaic and fluvial deposits of the Kern River Group. Moving into the late Pliocene there began a change in the principal depocenter of the SJB, from the area of the Maricopa basin and southern Kern Arch to the northern Arch and Tulare basin. With the Quaternary rise of the Arch, Tulare basin was left as a distinct Quaternary depocenter. The events which led to the migration of the principal depocenter, the uplift of the Arch and the persistence of the Tulare basin entailed the progressive southeast to northwest delamination of the underlying mantle lithosphere as discussed below.

Figure 13. Late Miocene paleogeographic map showing change in facies related to lithosphere break-up (see Figs. 17, 18 and 20), and the initiation of regional west tilting of the Sierra Nevada. Most notable is the production and deposition of the shallow marine plutoniclastic Santa Margarita sand sheet.

SELECTED REFERENCES

Atwater, T., and J. Stock, 1998, Pacific–North American plate tectonics of the Neogene southwestern United States: An update, International Geological Review, v. 40, p. 375-402.

Clark, M.K., Maheo, G., Saleeby, J., and Farley, K.A., 2005, The non-equilibrium (transient) landscape of the Sierra Nevada, California: GSA Today, v. 15, p. 4-10.

Le Pourhiet, L., Gurnis, M., and Saleeby, J., 2006, Mantle instability beneath the Sierra Nevada Mountains in California and Death Valley extension: Earth and Planet. Sci. Lett., doi:10.1016/j.epsl.2006.08.028.

Mahéo, G., J. Saleeby, Z. Saleeby, and K. A. Farley (2009), Tectonic control on southern Sierra Nevada topography, California, Tectonics, 28, TC 6006, doi:10.1029/2008TC002340.

Saleeby, J., and Foster, Z., 2004, Topographic response to mantle lithosphere removal, southern Sierra Nevada region, California: Geology, v. 37, p. 245-248.

Saleeby, J., Ducea, M.N., Busby, C.J., Nadin, E.S., and Wetmore, P.H., 2008, Chronology of pluton emplacement and regional deformation in the southern Sierra Nevada, California: in Wright, J.E. and Shervais, J.W. eds., Ophiolites, Arcs and Batholiths: A Tribute to Cliff Hopson, Geol. Soc. Amer. Sp. Pap. 438, p.397-428.

Saleeby, J., Saleeby, Z., Nadin, E., and Maheo, G., 2009, Stepover in the structure controlling the regional west tilt of the Sierra Nevada microplate: eastern escarpment to Kern Canyon system: in W.G. Ernst, Ed., Special Volume on the Nevada Plano, International Geology Review v. 51, n. 7-8, p. 634-669.

Stock, G.M., R.S. Anderson, and R.C. Finkel, 2004, Pace of landscape evolution in the Sierra Nevada, California, revealed by cosmogenic dating of cave sediments, Geology, v. 32, n. 3, p. 193-196, doi: 10.1130/G20197.1.

Zandt, G. Gilbert, H., Owens, T., Ducea, M., Saleeby, J. and Jones, C., 2004, Active foundering of a continental arc root beneath the southern Sierra Nevada, California: Nature, v. 43, p. 41-45.

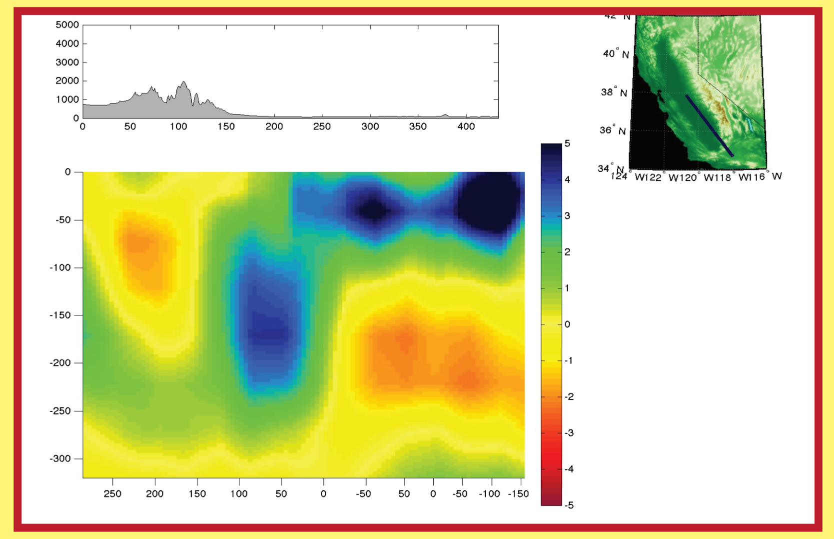

Figure 15. A sample of one of the P-wave tomographic sections used to generate the Figure 3 rendering of southern the Sierra mantle "drip." The tomographic sections were generated by SNEP-Sierra Nevada Earthscope Projects (in prep.). These sections show the mantle anomaly to be a SE to NE dipping slab that is attached up-dip the high-density mantle lithosphere that is still attached to the lower felsic crust.

Figure 16. Receiver function images across western Basin and Range-Sierra Nevada-eastern Tulare basin between 36°N and 37°N showing bright Moho where delamination has occurred, and a loss of the Moho where high-density mantle lithosphere is still attached to the lower crust. Also shown is E-dipping planar fabric that produces seismic anisotropy along delamination Moho, interpreted here as ductile shear zone. Hole in Moho is interpreted as area where lower crust is flowing into active delamination hinge (see Figs. 3, 15 and 18). These and additional RF sections were also used in Figure 3 rendering.

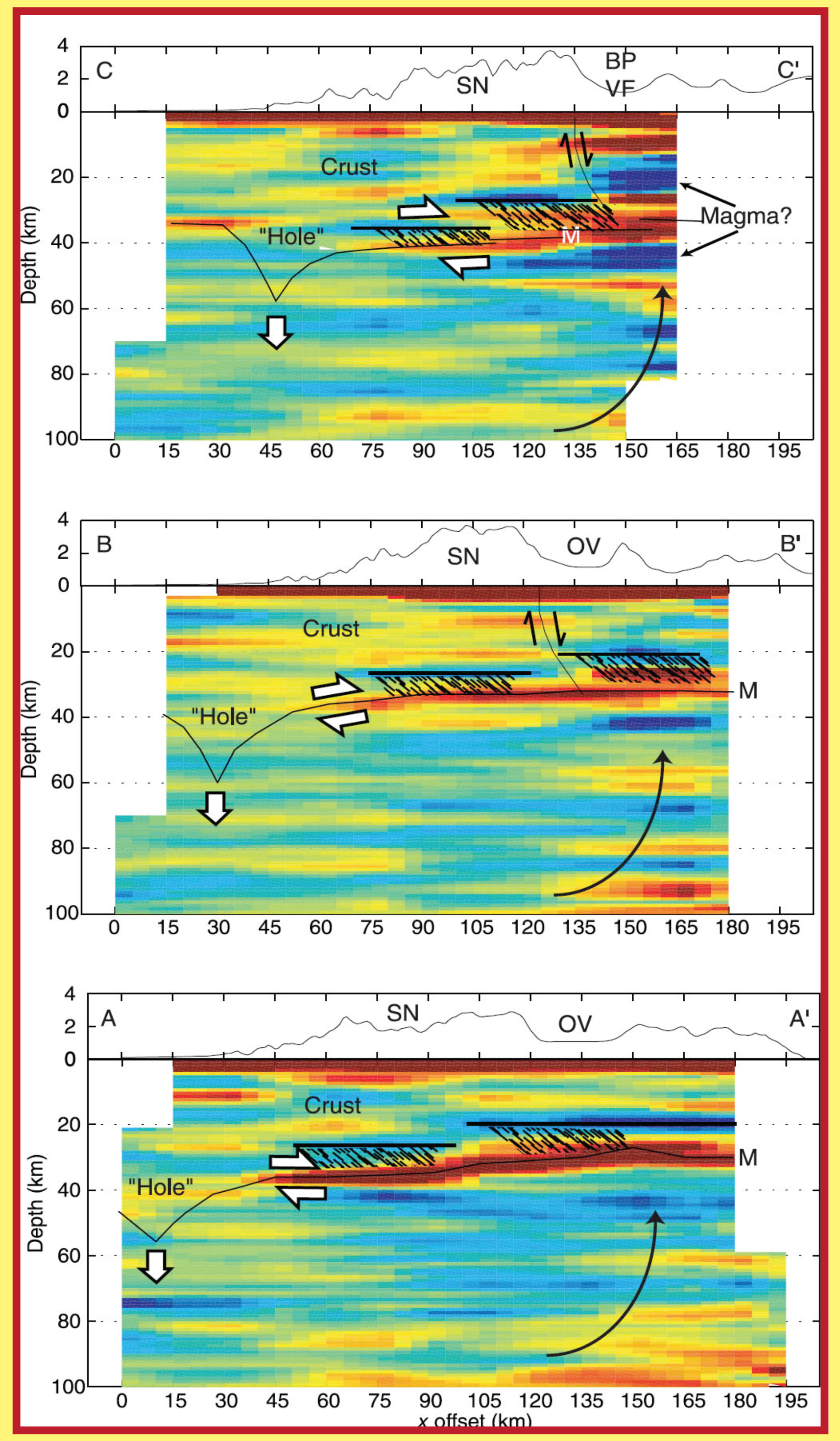

THERMO-MECHANICAL MODELING

We have constructed a series of thermo-mechanical models that entail visco-elasto-plastic thermo-dependant rheologies, and temperature and compositional dependence of density. Geological constraints on initial and boundary conditions employ mantle xenolith and lower crustal exposure compositional and thermo-barometric determinations as well as regional geologic structure. Plate kinematic constraints lead us to impose a slab window beneath the region at ca. 20 Ma, and a 5 mm/yr ~E-W extensional strain. Some specific goals of the modeling are to reproduce the geometry of the southern Sierra seismic velocity anomaly as imaged tomographically (Figs. 3 and 15), account for the flow of lower crust into the area of the mantle anomaly (Figs. 2 and 16), and explore the generation of geological structures and vertical displacements in the Earth's surface. The phase solution of the currently preferred model is shown in four time slices in Figure 17. Following a period of ~15 m.y. (20 to 5 Ma) of convective removal of lower peridotitic mantle lithosphere the upper eclogitic mantle lithosphere begins to delaminate from the lower crust. A critical event within this initial period occurs in the late Miocene (ca. 10 Ma) when lower crustal and mantle lithosphere regional low-angle ductile shear zones merge at Moho depths resulting in mantle lithosphere break-up instigating the eastern Sierra escarpment system and regional west-tilting of the Sierra Nevada (Fig. 13). This event is depicted in frames B to C in the dynamic solution to our currently favored model (Fig. 18). By ca. 4 Ma delamination is proceeding rapidly and at current time the model produces a southeast dipping, partially delaminated slab, that is still attached to the lower crust to the northwest (Figs. 3, and 15-18). In Figure 19 we show profiles of surface displacement along the model trace for 6, 3 and 0 Ma, and vertical displacement profiles of three critical points at the Sierra crest, western Foothills-Tulare basin transition and center of Tulare basin over the 15-0 Ma time interval. The Sierra crest pattern fits rock uplift data in time precisely based on cosmogenic dating of cave deposits along major southern Sierra river gorges. The Tulare basin and basin margin pattern fits tectonic subsidence patterns in the Tulare basin. Since delamination is proceeding in three dimensions (Fig.3), similar vertical displacement patterns are present in tectonic subsidence along the eastern SJB (Fig. 4). Due to geometric constraints a longitudinal model trace is not feasible along the eastern basin margin, but we are currently in the midst of testing three-dimensional models to further clarify the vertical displacement patterns across the Earth's surface. In the three dimensional model the Kern Arch sits in a similar (longitudinal) position as the Sierra crest sits in transverse section. Figure 20 shows a comparison between the model predicted vertical displacement of the Sierra crest to tectonic subsidence at the topographic crest of the Arch. The correspondence is close!

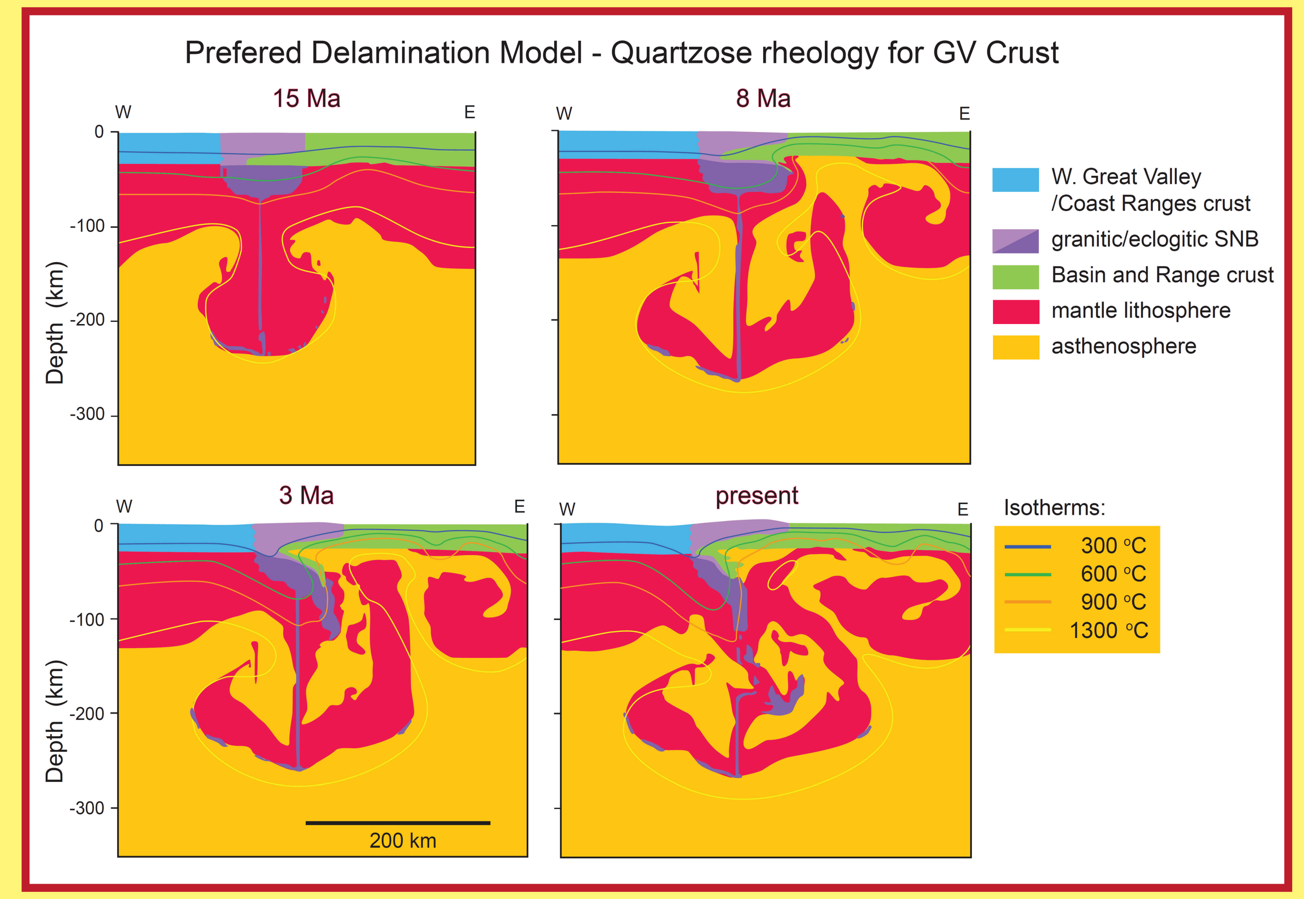

Figure 17. Phase solution of preferred thermo-mechanical model for mantle lithosphere removal beneath the southern Sierra Nevada region following ca. 20 Ma migration of slab window beneath the region. Convective removal of peridotitic mantle lithosphere preceded delamination of upper eclogitic mantle lithosphere.

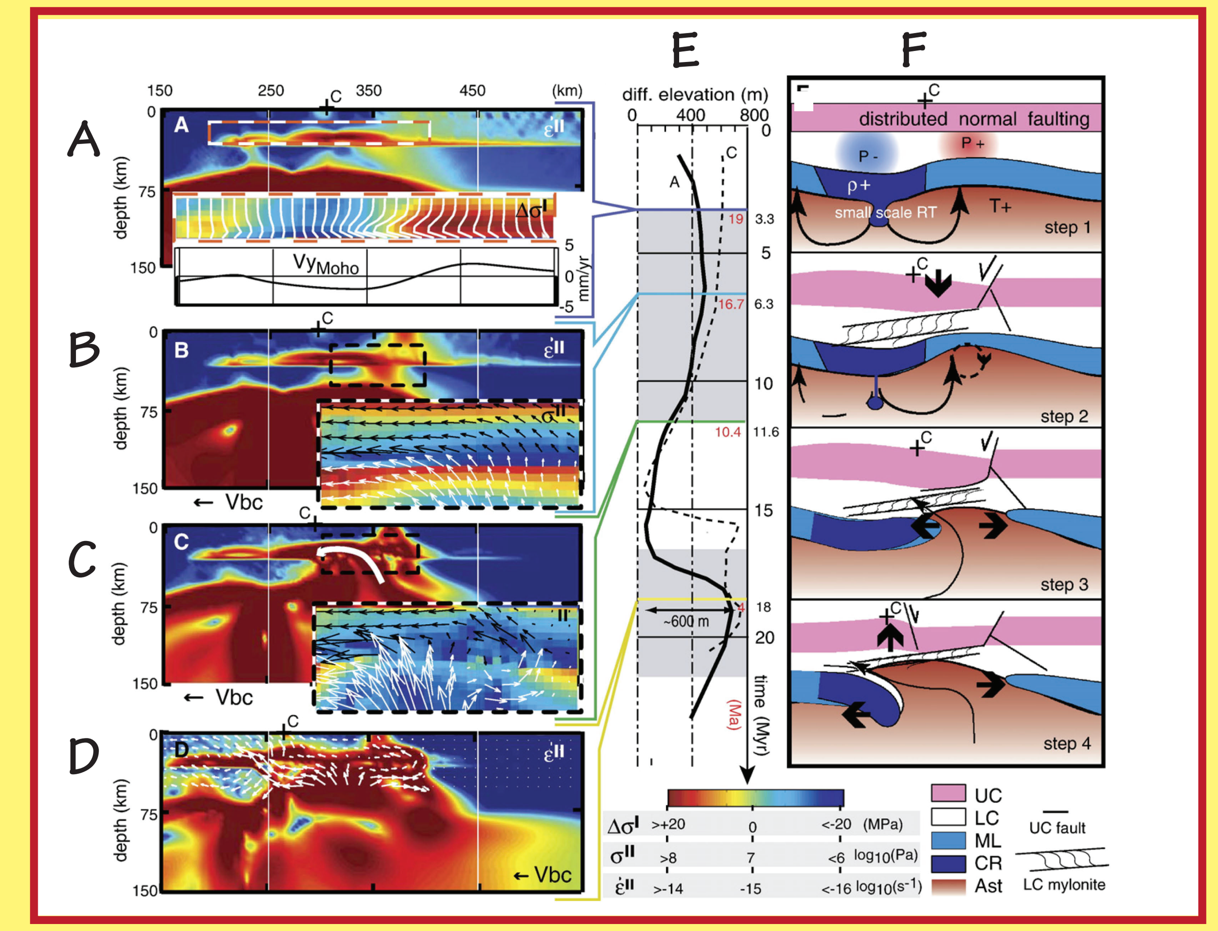

Figure 18. Dynamic solution of (preferred) thermo-mechanical model for mantle lithosphere removal (A-D). $\Delta\sigma^{I}$=dynamic pressure, σ^{II} =radius of Mohr circle, ε^{II}=shear strain rate, and Vy=vertical velocity at Moho. E shows predicted vertical displacement on current eastern Sierra crest with time and F shows cartoon of relations between surface extensional faulting, lithosphere break-off and delamination.

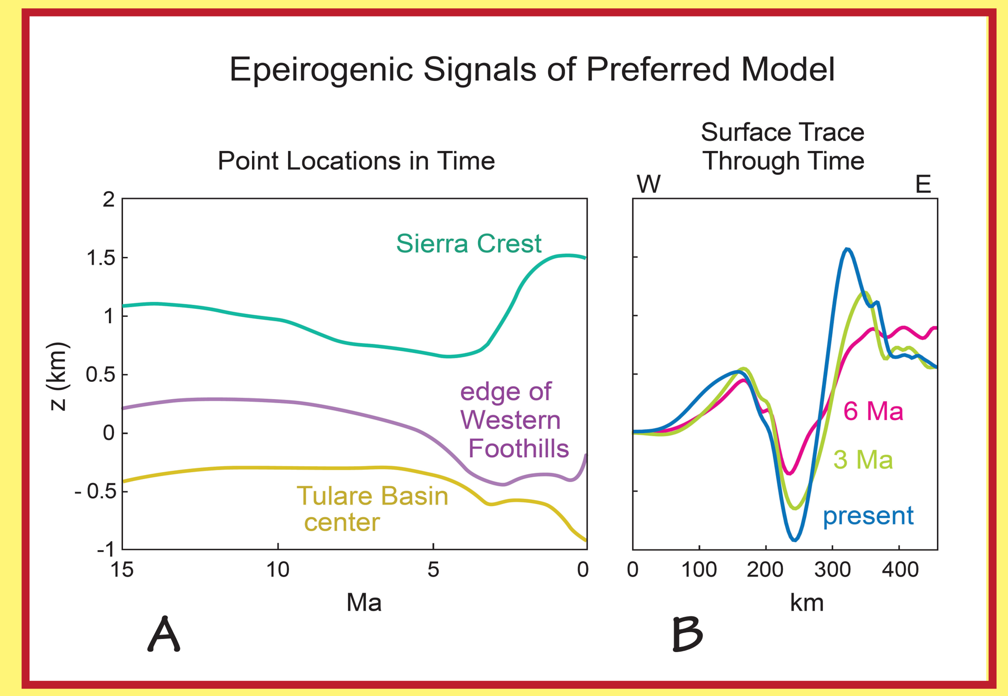

Figure 19. Vertical displacement profiles along model trace of Figures 17 and 18. A shows past 15 m.y. displacements for three critical points, and B shows vertical displacements along model trace for three critical points in time.

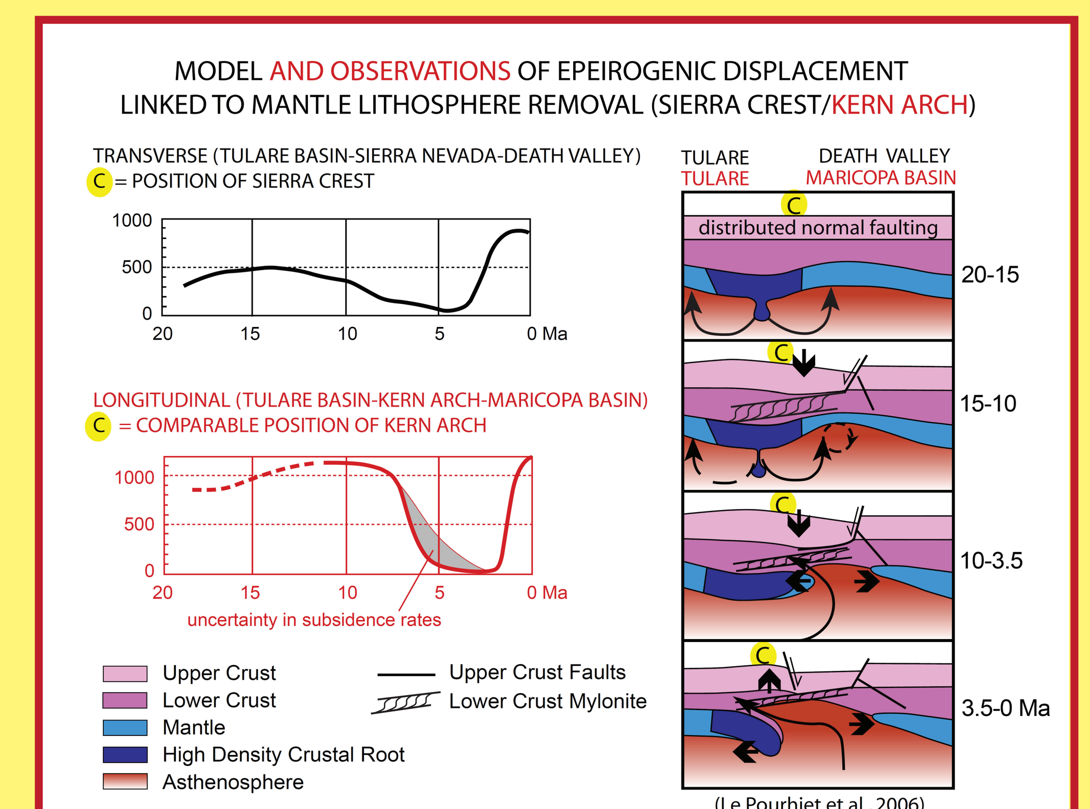

Figure 20. Comparison of predicted vertical displacement in time of a point lying on the current eastern Sierra crest (Fig. 18e) with tectonic subsidence history of point on the topographic crest of the Kern Arch. These two points sit in comparable positions relative to delamination hinge (Figs. 3 and 4). Cartoon along right margin shows delamination sequence from Figure 18f with comparable positions of Sierra and Arch crest and early to middle Miocene extensional terranes of Death Valley and the Maricopa basin.